Tribology International 189 (2023) 108901

Contents lists available at ScienceDirect

Tribology International

journal homepage: www.elsevier.com/locate/triboint

Fatigue lifetime prediction model for leading edge protection coating systems of wind turbine blades

T.H. Hoksbergen *, R. Akkerman, I. Baran

University of Twente, Drienerlolaan 5, Enschede, 7522NB, The Netherlands

ARTICLE INFO

Keywords:
Lifetime prediction
Leading edge erosion
Fatigue damage
Coatings
Wind turbines

ABSTRACT

Rain erosion of wind turbine blades causes increased maintenance cost and shortened intervals. Lifetime prediction of coating systems is challenging because of complexities in determining liquid droplet impact pressures, resulting coating stress history and high strain rate fatigue parameters. The current work discusses a novel modeling method for characterizing single point and distributed impact fatigue lifetimes. The effects of changes in material, impact and geometric parameters on the predicted lifetimes were studied. Droplet diameter and coating layer thickness were found to play an important role in the lifetime of the system. Overlap of stress histories led to a difference between single point and distributed impact location lifetimes. The resulting model allows more elaborate analysis of LEP performance.

1. Introduction

With global climate agreements driving the energy transition, sustainable electricity sources such as wind energy are becoming more important. Offshore wind has high potential to generate large amounts of electricity because of a larger swept area resulting from longer blades. Currently, the largest wind turbines have diameters over 200 m. These large turbines have blade tip speeds of over 100 m s^{-1}. The high speed tips interact with rain droplets and other airborne particles causing erosion damage over time [1]. Although the occurrence of rain erosion is well known nowadays in the wind energy sector, the fundamental understanding of the mechanisms driving rain erosion as well as predictive models need to be further developed. Leading edge protection (LEP) layers are commonly applied to the blades in order to protect them from erosion damage. These LEP systems can be applied directly in liquid form (gelcoats or polyurethane based coatings) or as tape/shell form by adhesive bonding. The performance of these systems is generally determined by extensive experimental test campaigns rather than predictive modeling based on common material parameters.

Fatigue lifetime is generally expressed by SN-curves containing the applied stress level (S) on the y-axis and the number of cycles to failure (N) on the x-axis. This relation is often fitted by a power law or logarithmic law. For rain erosion of wind turbine blade applications, often a VN-curve is used instead, which uses impact velocity (V) instead of stress. Since the number of stress cycles is not easily measured in the field or in whirling arm rain erosion test setups, often the lifetime is expressed as time before failure, specific number of impacts per area or impingement, which is the total impacted water column. These values can be converted into each other when the test conditions are constant. The conditions are different between single point impact tests and distributed impact point tests, which might result in variations in predicted lifetime. This further complicates the correlation between rain erosion tests and field data.

The traditional way to determine the liquid droplet impact erosion lifetime of a coated substrate is by using the Springer model [2]. This model defines a so called erosion strength based on the fatigue parameters of the material. The number of impact events before damage initiation (incubation) is calculated by fitting a power law to the ratio of the erosion strength to the impact pressure. For this impact pressure value, traditionally, the waterhammer pressure is used. The coefficients of the power law were found to be constant for most metallic and ceramic materials. Variations on the Springer model have been developed and used in the wind turbine blade industry [3]. Since recently, elastomeric materials are more often used as coating layers [4]. The Springer model is not able to accurately predict erosion lifetimes for these materials due to a singularity in the model for $\nu \rightarrow 0.5$ [5]. Often, this problem is overcome by assuming the power law coefficients to not be constant and by fitting them to experimental rain erosion test results. This fitting however is undesired since prediction of lifetimes is ideally based on material parameters and not on extensive experimental rain erosion testing.

* Corresponding author.
E-mail address: t.h.hoksbergen@utwente.nl (T.H. Hoksbergen).

https://doi.org/10.1016/j.triboint.2023.108901
Received 15 June 2023; Received in revised form 22 August 2023; Accepted 24 August 2023
Available online 30 August 2023

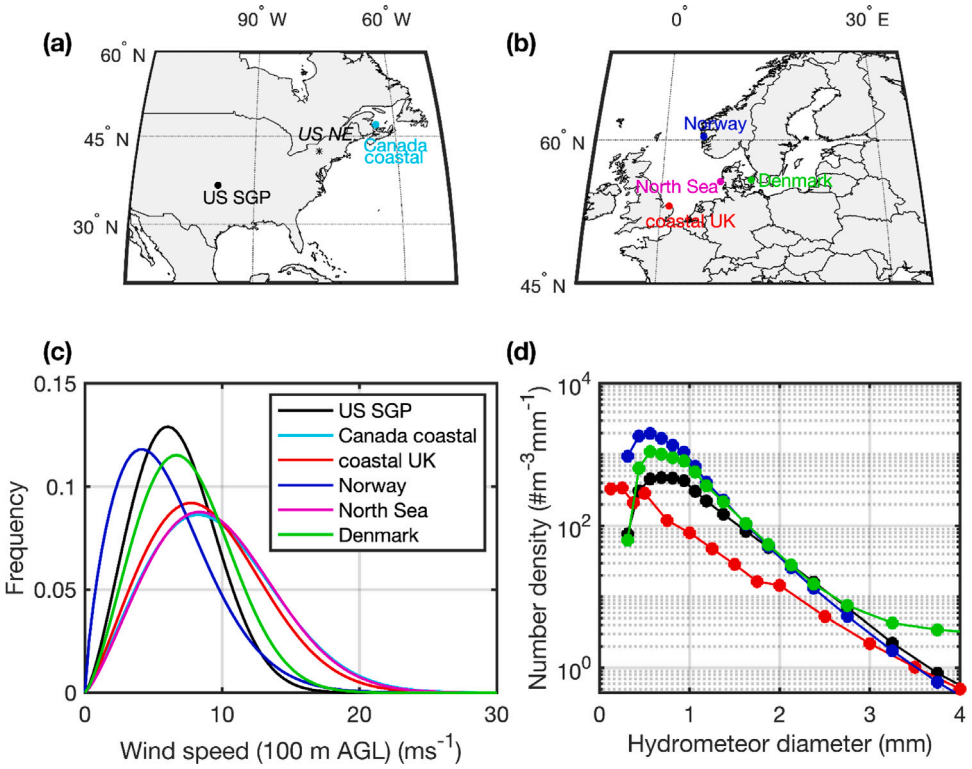

Fig. 1. Wind turbine sites in North America (a) and Europe (b) where site-specific wind velocity distribution (c) and droplet size distribution (d) were measured. *Source:* Reproduced with permission from Pryor et al. Energies; published by MDPI, 2022 [6].

An engineering approach to surface fatigue damage using the Palmgren–Miner fatigue damage rule was proposed for lifetime prediction of coated substrates by Slot et al. [7]. This approach considers a maximum surface stress based on the waterhammer pressure that depends on the radial coordinate caused by the Rayleigh wave. This stress is related to traditional fatigue material data by the Palmgren–Miner damage rule in order to define the increase in damage per hour. From this, the incubation time was calculated defined as the time when the damage parameter reaches unity. It was found that lifetime can be increased by reducing the contact pressure or enlarging the safe area by applying coatings with adjustable compressive stresses, adjustable hardness and a low amount of defects and impurities. In a follow up study, the SN–curves were determined for two different polybutylene terephthalate (PBT) materials from axial tension/tension fatigue tests (R = 0.1). This data was used with the model to successfully predict incubation times for these materials [8]. The model was extended with strain-hardening and shot peening for metallic surfaces which resulted in a good correlation with laboratory results for AISI 316 steel and AL6061-T6 [9]. The model has not yet been applied to more commonly used elastomeric LEP materials.

Where the previously discussed lifetime prediction models make use of the Waterhammer equation, numerical modeling has been applied to obtain a more accurate prediction of the pressures and stresses involved in liquid droplet impact. Numerical methods based on combined Eulerian–Lagrangian modeling as well as smoothed particle hydrodynamics [10,11] have been proposed. The modeled stresses have been used in combination with the Palmgren–Miner rule [12] or critical plane fatigue analysis [13] in order to predict lifetimes. The Rainflow counting method was used to track the stress cycle magnitudes and counts for dynamic, varying loads. The Rainflow counting algorithm does not directly consider the amplitudes of the different frequencies present in the stress signal, but the maximum stresses occurring as a result from these superimposed signals.

In order to accurately predict LEP lifetimes, it is necessary to include site–specific conditions in the modeling framework. Conditions such as wind speeds and droplet size distributions are taken into account by measuring and implementing meteorological data in lifetime prediction models [14,15]. These models are often based on empirical data and fitted to field observations. It was shown that droplet diameter and terminal velocity depend on the site [6] as shown in Fig. 1. Some numerical frameworks include the droplet size effect [16] to some extent.

Although it is generally assumed that droplet diameter affects the rain erosion performance, it was only recently shown by experiments [17]. It was found that droplet size affects rain erosion performance by the use of a whirling arm rain erosion test. The specific impacts, specific impacts per area and impingement values were computed and compared for four different droplet diameters and the resulting VN-curves were used to predict lifetimes for different meteorological sites. Predictive modeling efforts based on material parameters to study the effect of droplet diameter on predicted lifetime were not performed in this study and the current work could contribute towards a better fundamental understanding of the effect of droplet diameter on the stress and lifetime.

For polymeric materials at high strain rates it has been shown in literature that, the yield strength increases and the response in the glassy regime is linear up to a higher stress [18,19]. This indicates that for the high strain rates of liquid droplet impact, the stress response of the materials can be modeled using a linear elastic approach and the fatigue damage occurs in the elastic region. High-cycle fatigue methods that consider low stresses in the linear elastic regime should therefore be used. Although high–cycle fatigue is well known, the strain rate dependency for polymeric materials has not been studied extensively. Moreover, for high–cycle fatigue, initial defects become more important as damage nucleation points. Using fatigue data measured at low strain rates is therefore not recommended for accurate lifetime predictions, but it can be useful to study the trends of changes in impact, material and geometric parameters on the predicted lifetime.

This paper aims to develop a lifetime prediction model using numerical simulations based on the physical phenomena involved in liquid

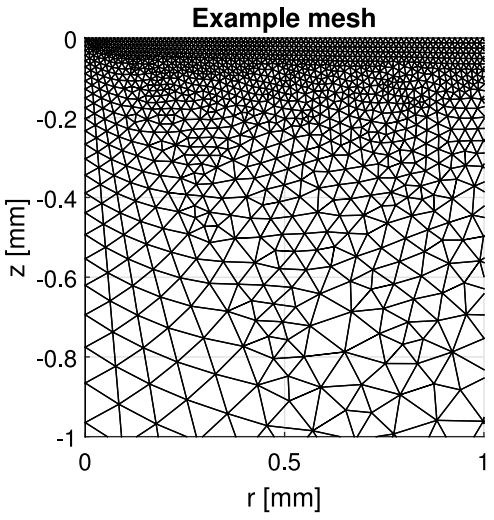

Fig. 2. Example of a part of a mesh for a bulk LEP material. The contact pressure is put as a pressure load at the top of the mesh. The transient problem is solved axisymmetrically for the radial coordinate (r), the depth (z) and time (t).

droplet impact that predict contact pressures and coating-substrate stresses. The method discussed takes into account a numerical framework including air cushioning [20,21] and is based on traditional fatigue damage modeling methods such as the Palmgren–Miner rule. As discussed previously, high–cycle, high strain rate ($\pm 10^6$ s^{-1}) fatigue parameters are ideally used. Since these are generally not readily available, the fatigue strengths used in this work are based on low strain rate experiments which does allow for prediction of the trends caused by changes in parameters, but not for accurate prediction of lifetimes. Moreover, for polymeric based coating systems, viscoelastic heating of the specimens occurs when the test frequency is high which influences the results. The effect of changes in impact, geometrical and material parameters on the resulting lifetimes will be discussed. The sensitivity of the lifetimes with respect to fatigue strength parameters will also be addressed. The model is developed with the aim to close the gap between rain erosion testing and modeling. This will allow a more accurate prediction of LEP performance and opens up the possibility to optimize LEP systems for use as protection layers against rain erosion damage for wind turbine blades.

2. Methods

The lifetime prediction model discussed in this paper uses the liquid droplet impact pressure including air cushioning [21] and a slight adaption of the coating stress model [20] proposed in earlier work by the authors. Axisymmetry is used to allow for extensive parameter studies within acceptable computation times. The Von Mises stresses are considered for the damage calculations in this work but other stress components can be used in the analysis as well. The resulting stress history $\sigma(r, z, t)$ is stored for each node in the mesh of which an example is shown in Fig. 2. An example of the stress history for a 2 mm water droplet impacting a flat epoxy panel at 100 m s^{-1} is shown in Fig. 3 and can be obtained from the supplementary dataset [22]. It can be seen that the stresses in the target rise when the pressures increase at the instance of contact at 1 μs. The high stress regions disperse relatively fast and mainly the initial contact is important for the high stress state due to the compressive effects in the droplet.

The algorithms developed in this work were implemented in Matlab® using the Rainflow counting algorithm provided in the signal processing toolbox which follows the ASTM E1049-85 standard [23]. Rainflow counting can be applied for data reduction of the full stress history in each node to a filtered set of discrete load changes (thus their average and amplitude) and their number of occasions, which can subsequently be used with Miner's rule to determine the resulting nodal damage parameter. Note that the damage parameter in Miner's rule is based on an elastic analysis and varies between 0 and 1 where a value of 1 indicates that the material is damaged. The current approach does not include damaged geometries in the numerical analysis. The developed Matlab code and a required stress input file are published as a supplementary dataset to this paper [22]. The stress input file is obtained by means of a transient axisymmetric FEM simulation [20] which uses a pressure input solved from an axisymmetric two-phase flow fluid–structure interaction droplet impact simulation [21].

In order to calculate lifetimes, a material strength model is required. The strength parameters used for the present analysis were based on a power law according to

$$N_f(\sigma) = \left(\frac{\sigma}{\sigma_U}\right)^{-\frac{1}{m}}, \text{ where } m = -\frac{\log(N)}{\log(\sigma_I) - \log(\sigma_U)} \tag{1}$$

where σ is the stress level, σ_U is the ultimate tensile strength, σ_I the fatigue limit at N cycles and N_f the lifetime at stress level σ. This damage law is linear in a graph with logarithmic axes. Fig. 4 shows the SN-curve for Eq. (1) for an epoxy material as defined in Table 1. The endurance limit is implemented as a cut-off below which damage accumulation does not occur. This results in a knee in the fatigue curve as indicated in the figure by the dashed line. The proposed damage model is used in a parameter study of the trends in the resulting VN-curves.

The following subsections discuss lifetime calculations for impacts occurring in a single point and at distributed impact locations respectively. Although the same building blocks are used for the calculations, the interpretations are slightly different. For the remainder of this work, calculated lifetimes are denoted by a bar and Rainflow counting variables by a tilde. The stress values used as input are based on a slight adaption of the coating stress model [20] which used a triangular mesh.

2.1. Single point impact method

For impacts occurring at a single point, the extracted stress history for a single impact event was used in the Rainflow counting algorithm to obtain the number of stress cycles and the magnitudes that each point in the LEP system endured. As shown by the stress history in Fig. 5, the signal can contain multiple stress cycles that have to be considered by the Rainflow counting algorithm. The Palmgren–Miner rule was used with the stress cycle magnitudes and counts to determine the damage parameter for each point. The point with the highest damage parameter is considered as the point where damage initiates. By taking the inverse of the damage parameter, the expected lifetime can be obtained as the number of impacts before damage for single point impacts. Since this method directly relates to the stress history, it is a deterministic approach.

The following summarizes the lifetime calculation method for single point impacts:

1. Perform Rainflow counting to obtain the stress cycle amplitudes ($\tilde{\sigma}_j(r, z)$) and the number of stress cycles at each stress level ($\tilde{N}_j(r, z)$) for each node in the stress history data. Note that both have a length $\tilde{n}(r, z)$ representing the distinct number of stress levels distinguished in the signal, denoted by the subscript j.
2. Calculate the damage parameter D for each node from the Rainflow counting data according to:

$$D(r, z) = \sum_{j=1}^{\tilde{n}(r,z)} \frac{\tilde{N}_j(r, z)}{N_f\left(\tilde{\sigma}_j(r, z)\right)} \tag{2}$$

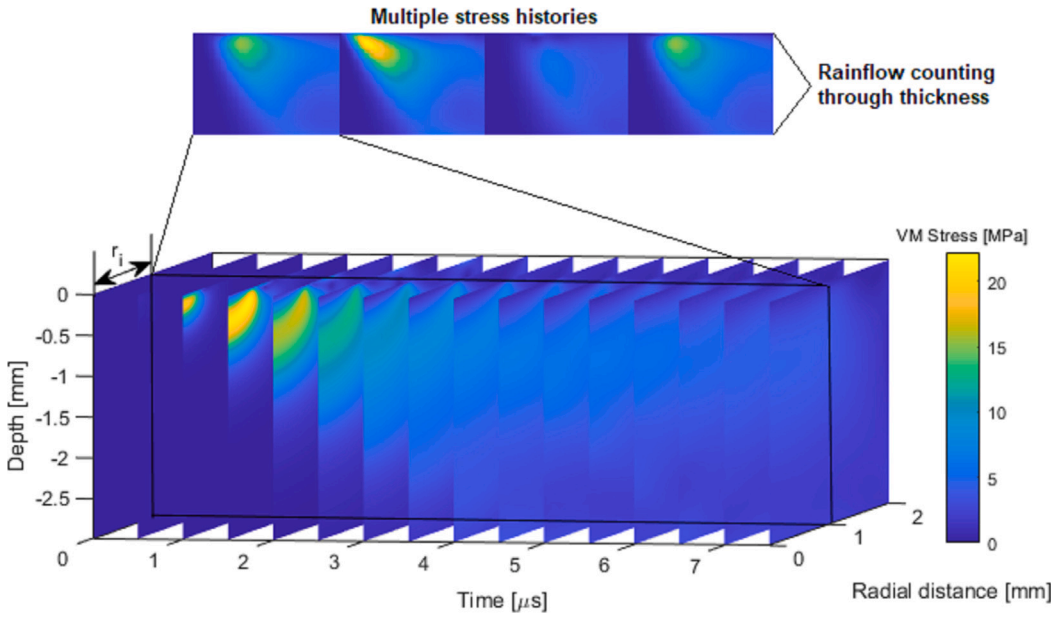

Fig. 3. Stress history for a 2 mm diameter water droplet impacting an epoxy material at 100 m s^{-1} and the extraction method for distributed impact location stress history.

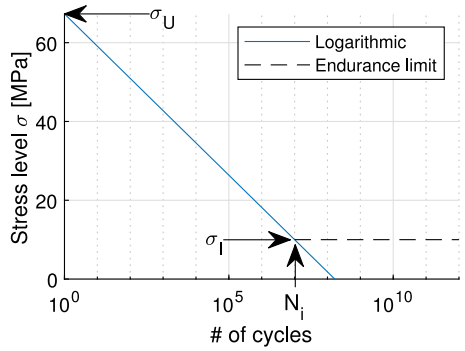

Fig. 4. Model used for fatigue SN–curve interpretation and the endurance limit based on Eq. (1) and the material parameters of epoxy in Table 1 with $R = -1$.

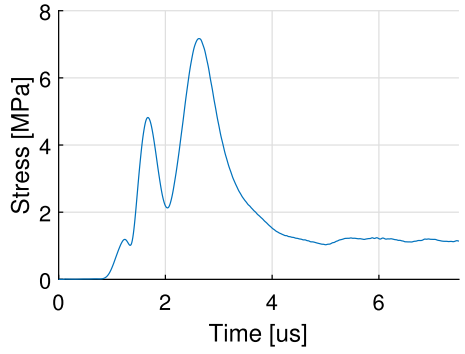

Fig. 5. Stress history at a node resulting from a single impact event containing multiple stress cycles to be considered by Rainflow counting.

3. Calculate the lifetime in number of impacts ($\bar{N}_i^*$) for each node by:

$$\bar{N}_i^*(r,z) = \frac{1}{D(r,z)} \tag{3}$$

This analysis results in a two dimensional figure containing the damage parameter for each node. The node with the lowest lifetime value will be the location where damage is expected to initiate and the resulting lifetime value is considered as the lifetime of the material system.

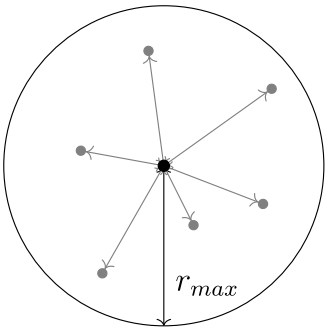

Fig. 6. Schematic representation of the calculation for the distributed impact location distribution with six impact points with distances r_i towards the point of interest in the center.

2.2. Distributed impact locations

Lifetime prediction for distributed impacts is more complex since the stress histories from different locations need to be superimposed. Because of the random nature of the superposition, this method is stochastic. In order to calculate lifetimes for distributed impact locations, a single point is considered for the damage calculation and an impact location distribution (r_i) is determined for a number of impacts (n) around this point by

$$r_i = r_{\max}\sqrt{\mathrm{rand}(n)} \tag{4}$$

where $\mathrm{rand}(n)$ is an array of n numbers between 0 and 1 and $r_{\max}$ is the maximum distance to the point of interest to consider (generally taken as the width of the substrate in the simulation). This approach is schematically represented in Fig. 6.

The distances r_i are used to extract the stress history as represented in Fig. 3. The method is valid if at $r_{\max}$ the stresses have dispersed significantly and no longer contribute to damage. It is assumed that the stress fields of consecutive impacts do not overlap. Or, in other words, that the energy of a single impact event is dispersed before a second

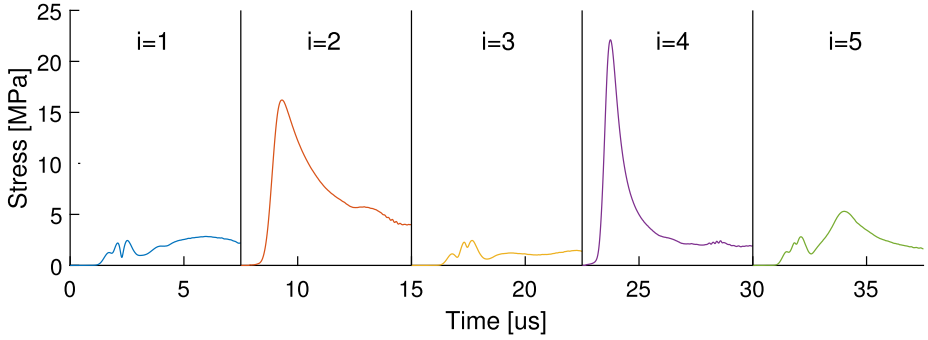

Fig. 7. Schematic representation of the construction of a continuous signal by concatenating signals from 5 discrete impact events at random locations.

impact occurs in the same region. From Fig. 3 it can be seen that the stress field does not extend beyond the droplet diameter (of 2 mm) and that the time in which it disperses is significantly smaller than 7.5 μs. This indicates that two droplets have to be very close together and have to impact within a few microseconds in order for their stress fields to interact. As a simplification, the average distance between two droplets of 2 mm diameter (d) for a rainfall rate (RR) of 10 mm/h with a uniform distribution and a terminal velocity (V_t) of 6 m s^{-1} was calculated. This was done by calculating the number of droplets in a cubic meter (N_d) as:

$$N_d = \frac{0.001RR}{3600V_dV_t}, \text{ where } V_d = \frac{1}{6}\pi d^3 \tag{5}$$

The inverse of this number is the volume of air that surrounds each droplet. By assuming the droplets to be packed closely like a face centered cubic lattice structure (with a packing factor of 74%), the minimum distance between two droplets is calculated by

$$d_{min} = \sqrt[3]{\frac{0.74 \cdot 6}{N_d\pi}} \tag{6}$$

which results in a minimum distance between two droplets of 0.2338 m for the given parameters. This indicates that the stress fields for two droplets impacting simultaneously do not interact. When the LEP velocity is assumed to be 100 m s^{-1}, the time in between two impacts for droplets in this uniform distribution at the same location is calculated by $t = r_{avg}/V$ to be 2.3 ms. In this time, the stress waves have dispersed significantly and do not interact as seen from the stress wave decay in Fig. 3. Based on this simplified analysis, it can be reasonably assumed that interaction between the stress fields of two consecutive impacts is negligible.

In order to predict the damage parameter and resulting lifetime for impacts that occur at distributed distances r_i from the point of interest, the stress histories at these distances have to be taken into account. For this purpose, the interpolated through thickness stress histories at n points at distances r_i from the center of impact are used in the Rainflow counting algorithm. This approach is represented in Fig. 3 by the extracted time histories at the top of the figure. This results in the stress cycle magnitude and count for the set of impact locations distributed around the point of interest as a function of the z-coordinate. The resulting damage parameter and expected lifetime therefore take into account distributed impact locations. For simplicity, the method proposed in this work uses a constant droplet diameter but the model can easily be adapted to take into account droplet sizes according to a well defined droplet size distribution (DSD) or disdrometer data accounting for site specific conditions.

The following summarizes the approach developed for lifetime calculation due to distributed impacts:

1. Determine a set of discrete droplet impact locations r_i according to:

$$r_i = r_{max}\sqrt{\text{rand}(n)} \tag{7}$$

where rand(n) is an array of n randomly distributed floating point numbers on the domain $[0, 1]$.

2. Interpolate and concatenate the stress histories $\sigma_i(r, z, t)$ from n distributed impacts at distances r_i from the center ($i = 1 \dots n$) to a combined stress history distribution through the thickness at the respective distances $r = r_i$ according to

$$\sigma(z, (i-1)\Delta t + t) = \sigma_i(r_i, z, t) \quad t \in [0, \Delta t],\ i = 1 \dots n \tag{8}$$

where Δt is the duration of a single impact. Note that this equation forms a continuous signal from discrete events. This is schematically represented in Fig. 7 for 5 signals at a single z-coordinate and in Fig. 3 for 4 signals through thickness.

3. Perform Rainflow counting on the resulting stress signal ($\sigma(z, t)$) to obtain the stress cycle magnitudes ($\tilde{\sigma}_j(z)$), the number of cycles at each stress level ($\tilde{N}_j(z)$) and the distinct number of stress levels $\tilde{n}(z)$. Note that for distributed impacts, these variables are only a function of the z-coordinate and not of the r-coordinate.
4. Calculate the damage parameter D as a function of the z-coordinate from the Rainflow counting data according to:

$$D(z) = \sum_{j=1}^{\tilde{n}(z)} \frac{\tilde{N}_j(z)}{N_f\left(\tilde{\sigma}_j(z)\right)} \tag{9}$$

Because the concatenated stress history $\sigma(z, t)$ was taken into account, the damage is a result of n impacts in a circular area with radius r_{max} as was shown in Fig. 6.

5. Calculate the lifetime as specific impacts $\bar{N}_A$ and impingement $\bar{H}$ according to:

$$\bar{N}_A(z) = \frac{n}{D(z)A}, \text{ where } A = \pi r_{max}^2 \tag{10}$$

and

$$\bar{H}(z) = \bar{N}_A(z)V, \text{ where } V = \frac{4}{3}\pi r_d^3 \tag{11}$$

Since the approach for distributed impact locations is stochastic, the calculations can be performed multiple times to determine the mean and standard deviation of the predicted lifetime. These values can be used to optimize the number of impact locations considered n. It was found that a value of $n = 5.000$ leads to a good balance between results and computation time.

2.3. General problem definition

In order to predict VN-curves, the developed approaches can be repeated for multiple impact velocities and the resulting lifetimes can be plotted as a function of impact velocity. The discussed approaches also allow for studying the effect of droplet diameter, material parameters, layer thicknesses and other impact, geometrical and material parameters on the predicted lifetimes of the coating-substrate systems.

For this work, coated-substrates are considered as leading edge material systems. An interphase region is present between the two

Table 1
Material parameters considered for the coating materials used in the current work.

Material	TPUD60	Epoxy	PAI
E [GPa]	0.25	2.41	4.9
ν [–]	0.4575	0.399	0.45
ρ [kg m^{-3}]	1100	1255	1425
σ_U [MPa]	55.1	67.3	192
σ_I [MPa]	10	10	10
N [–]	10^7	10^7	10^7

Table 2
Impact and geometric parameters considered for the simulations in this work.

V [m s^{-1}]	d [mm]	h_{LEP} [μm]	h_{IP} [μm]
80	1	250	**0**
100	**2**	500	50
120	3	750	100
140		∞	
160			

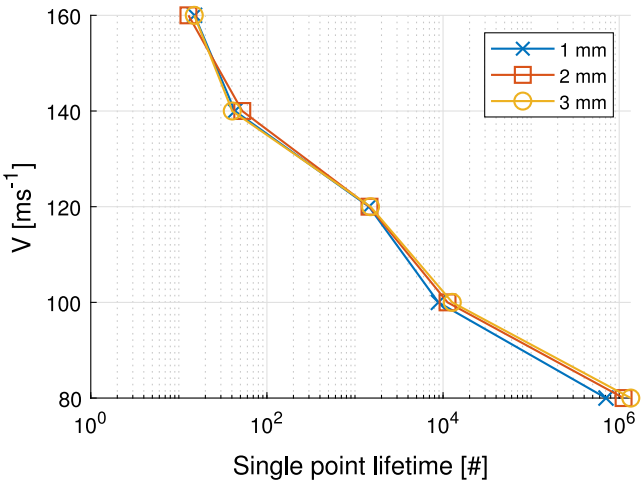

Fig. 8. The effect of droplet diameter on the predicted lifetime of an epoxy target for a single impact location.

materials where the material properties gradually change. The effects of material parameters, droplet diameter, impact velocity and LEP thickness and interphase thickness on the predicted lifetime will be discussed. The material parameters considered in this work are given in Table 1. The epoxy material properties are also used for the substrate since the properties in the thickness direction are driven by the substrate.

The impact and geometric parameters considered for the simulations in this work are summarized in Table 2. V is the impact velocity, d the droplet diameter, h_{LEP} the LEP thickness and h_{IP} the interphase thickness. The bold settings are used as a reference case. The infinite LEP thickness means that the coating was modeled as a bulk material without a glass-epoxy substrate underneath. Note that the interphase layer was modeled as a functionally graded material in order to obtain the stress field, but that the strength properties of the interphase region were unknown. Therefore, strength and fatigue life were determined only in the pure LEP layer based on low strain-rate fatigue properties. This is a limitation of the current modeling approach but it is still valuable to evaluate the developed method and to study the trends of changes in parameters on the predicted lifetimes.

In order to effectively take into account fatigue damage through thickness for distributed impacts, a number of points in z–direction had to be considered. Within the LEP layer, at least 50 points were used for the damage calculation through thickness. When this resulted in elements larger than 10 μm, the size was limited to 10 μm. In the substrate, the distance between the points was set to 100 μm. When a single material was used, the size of 10 μm was used for the top 1 mm. An increase of resolution was possible but would result in a computationally more expensive Rainflow calculation. Fortunately, this calculation only had to be performed once for each simulation since the stress levels and number of cycles were stored. The strength parameters could be changed/fitted to the stored data which is computationally more efficient.

3. Results

The lifetime calculations performed for this work follow the approaches described in the methods section and the resulting VN–curves are plotted and the effects of changes in parameters are discussed. For convenience, the process of calculating a VN–curve for both single point impact and distributed impacts is demonstrated once below.

For single point impacts, the stress history (from e.g. Fig. 3) is used directly in the Rainflow counting method to obtain the stress cycle magnitude and count for each node. From the stress magnitudes and counts, the damage parameter is calculated per node according to Eq. (2). The result is the damage that occurs as a function of a single impact in each node. In order to calculate the lifetime, the maximum damage value is extracted as D_{max}. The number of impacts before the damage parameter equals one can now be calculated by taking the inverse of D_{max}. This gives the lifetime in number of impacts for a certain set of input parameters as $\bar{N} = \frac{1}{D_{max}}$. Repeating this process for multiple impact velocities results in a VN–curve. Note that for single point impacts with equal droplet size and velocity, the stress history in each node is repeated for each impact and that damage initiation therefore occurs in the point with the highest damage parameter from a single impact.

For distributed impacts, the stress history is not constant. This complicates the lifetime calculation because the stress history has to be determined accordingly. A set of impact distances r_i to the point of interest (in which damage is determined) is calculated based on Eq. (4). The stress history that is felt for each of these impacts at the point of interest can be determined by extracting the stress history at a distance r_i from the center of impact as shown in Fig. 3. The interpolated stress history at these distances is calculated for a number of impact points n (set to equal 5.000) and used in the Rainflow counting method. This results in stress cycle magnitudes and counts resulting from n distributed impacts for the point of interest for multiple z-coordinates. Similar to the approach for single point impacts, the damage parameter can be calculated from the stress cycle magnitudes and counts. In this case, the damage parameter is constructed from multiple impact histories and not based on the history in a single node. Note that this parameter is obtained for multiple z-coordinates leading to a profile of the accumulated damage through the thickness. Because this analysis takes into account a certain area A and a certain number of impacts n, the lifetime follows from Eq. (10) to obtain the number of impacts per square meter or Eq. (11) to obtain the impacted water column (or impingement). Note that the relation with the number of impacts for single point impacts is not trivial since the stress field size and shape cause a complex overlap for which the coupling is based on the discussed approach. It is not possible to state an influenced area for single point impacts and hence, it is not possible to determine the impingement value or specific impacts for single point impact locations. Since single point impact methods correspond with (most) jet based rain erosion tests while the distributed impact method corresponds with traditional rain erosion tests and field data. Both are considered in this work. Because of this, the analyses in this work are separated for single point impact locations and distributed impact locations in the following sections. The sensitivity of the model to changes in fatigue strength parameters is investigated and reported in a third section.

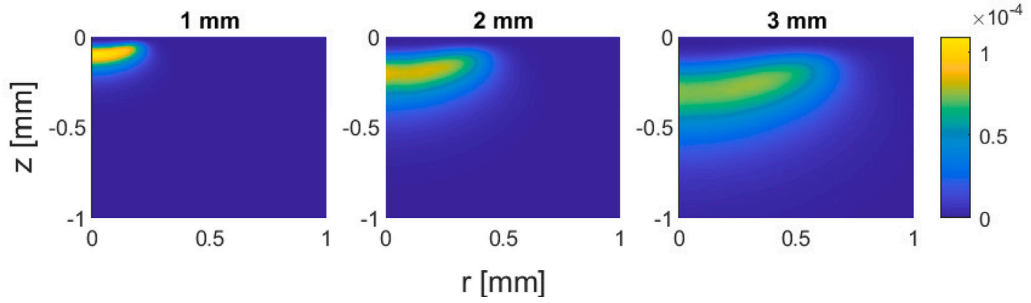

Fig. 9. Damage parameter for each node representing the damaged area and depth for single point impacts on epoxy targets at 100 m s^{-1} for different droplet diameters.

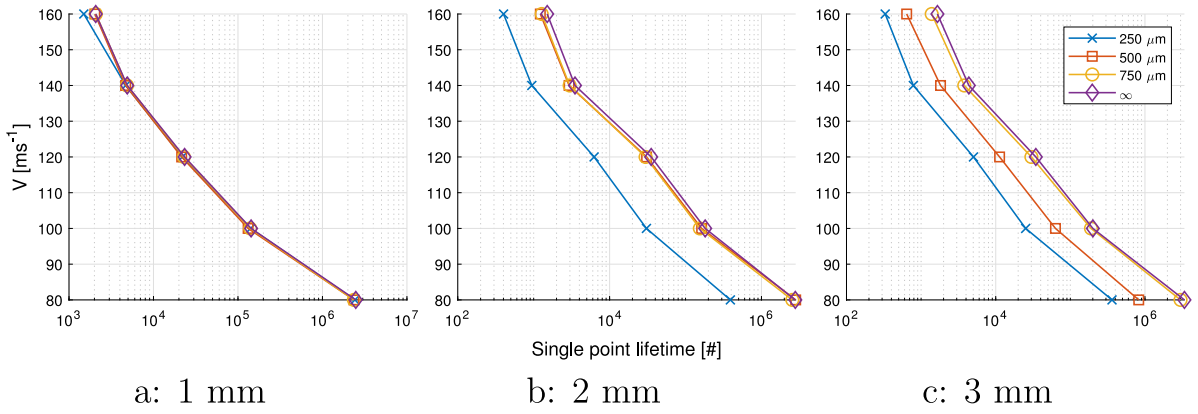

Fig. 10. The effect of LEP thickness on the predicted lifetime of PAI coated epoxy substrates for different droplet diameter impacts at a single location.

3.1. Single point impacts

The effect of droplet diameter on the predicted lifetime of bulk epoxy targets is shown in Fig. 8. It can be seen that the effect of droplet diameter on the predicted lifetime is very limited. All three curves do however show a deviation for an impact velocity of 120 m s^{-1}. It was found that for all three droplet diameters, the maximum stress at this impact velocity shows the same trend. Therefore, this is expected to be related to the stress history, and not the lifetime prediction method. When observing the damage depth and area given for an impact velocity of 100 m s^{-1} in Fig. 9, it can be observed that the depth at which the damage occurs is predicted to be slightly larger for larger droplets. Also, the affected area is significantly larger for larger droplets. Note that the color scale is linear and the lifetime is given in logarithmic scale. For single point impacts at an epoxy target, it is therefore expected that the damage will initiate around the same number of impacts independent of the droplet diameter. For larger droplets however, the expected damaged area is predicted to be larger.

Fig. 10 shows the effect of droplet diameter and LEP thickness on the predicted lifetime for a PAI coated epoxy substrate. It can be seen that for small droplet diameters, LEP layer thickness does not play a major role in the lifetime prediction. For larger droplets, LEP thickness plays a more important role where thicker LEP layers result in longer predicted lifetimes. This is due to the larger volume with high stresses that is present for larger droplets which interacts with the interface for thicker LEP layers. This figure therefore clearly illustrates that LEP thickness and droplet diameter are both important design parameters in lifetime prediction. Since droplet diameters are not constant and vary for each wind park site, the LEP solution should also be site specific and based on a sophisticated DSD or disdrometer data. A thicker LEP is generally beneficial in order to obtain a safe operation.

The effect of interphase thickness for single droplet impact locations on TPUD60 and PAI materials for 3 mm droplet impact on a 250 μm coated epoxy substrate is shown in Fig. 11. The materials are not compared to each other due to the absence of reliable high strain rate fatigue data. The figure clearly shows that interphase thickness has an effect on the lifetime of the LEP where thicker interphase regions lead to longer lifetimes. This is because the energy density in the stress wave is gradually reflected by the interphase which leads to lower stress concentrations for thicker interphases. Note that interphase thickness plays a significant role for thin LEP layers and not so much for thicker LEP layers. This is due to significant dispersion of energy density in the wave before it reaches the interphase for thick LEP layers. This leads to lower reflected stresses and hence, a lower effect of interphase thickness on the predicted lifetime for thicker LEP layers.

3.2. Distributed impact locations

For distributed impacts, the specific impacts and impingement values will be used. These values will be significantly different from the single point impact values and there is no trivial way to compare them. This does result in a shift on the x–axis of the VN–curves.

The specific impacts and impingement curves showing the effect of droplet diameter on the resulting lifetime of an uncoated epoxy target for distributed impact locations are given in Fig. 12. When considering specific impacts, it can be seen that the lifetime decreases for larger droplets, which has also been observed in experiments by Bech et al. [17]. This means that less large droplets are required to impact within a certain area in order for damage to accumulate at the leading edge. When observing the impingement value (impacted water column height), it can be seen that larger droplets lead to a longer lifetime and smaller droplets lead to an earlier onset of damage. This has to do with the fact that larger droplets have a higher volume and the impingement value increases faster than the damage due to the number of impacts. Since the maximum stress state is driven by the initial contact, generally it can be said that smaller droplets lead to an earlier accumulation of damage since more impact events occur for the

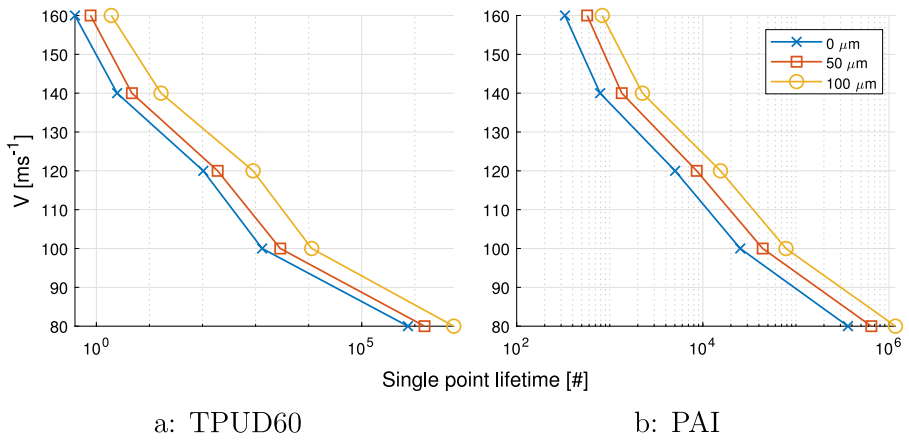

Fig. 11. The effect of interphase thickness on the predicted lifetime of 250 μm TPUD60 and PAI coated epoxy substrates for 3 mm droplet diameter impacts at a single location.

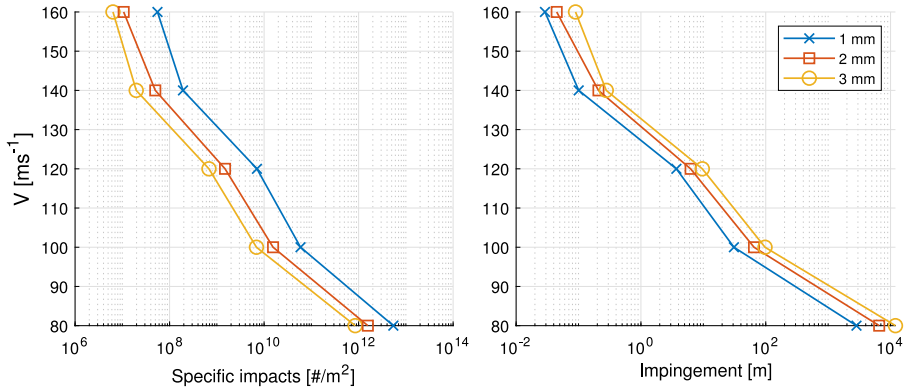

Fig. 12. The effect of droplet diameter on the lifetime of an epoxy target.

same impingement value. However, for larger droplets the affected area increases and overlap of lower stress cycle regions can occur increasing the number of fatigue cycles. So, although for single point impacts the predicted lifetimes for different droplet diameters were the same, for distributed impacts there is a non-linear effect caused by overlap of stress histories that significantly affects the predicted lifetimes both in terms of specific impacts as well as impingement. This effect clearly demonstrates why the relation between single point impact lifetime and distributed impact lifetime is non-trivial.

Fig. 13 shows the damage depth for distributed impacts on an epoxy target. From this figure, it can be seen that larger droplets cause damage deeper inside the material which is related to overlap of high stress regions. Moreover, the damage parameter is high in a larger region for larger droplet diameters which is related to the influenced area.

The effect of LEP thickness on the resulting lifetime highly depends on the stress state in the material and therefore also depends on the diameter of the impacting droplets. Fig. 14 shows the effect of LEP thickness on the impingement value of PAI coated epoxy substrates for 1 mm, 2 mm and 3 mm diameter droplets. It can be seen that in all cases thinner LEP layers led to a decreased predicted lifetime. This is expected because of the stress increase in the LEP layer due to reflections at the interface [20]. It can also be seen that for smaller droplet diameters, the effect of LEP thickness on lifetime becomes less for higher LEP thicknesses. For larger droplets, the effect is more prominent and thicker LEP layers result in significantly longer lifetimes. This is due to the larger volume of high stress and the resulting reflections at the interface. In general, thicker LEP layers have better performance. Based on the developed model, an LEP thickness limit can be derived for a certain set of impact and material parameters.

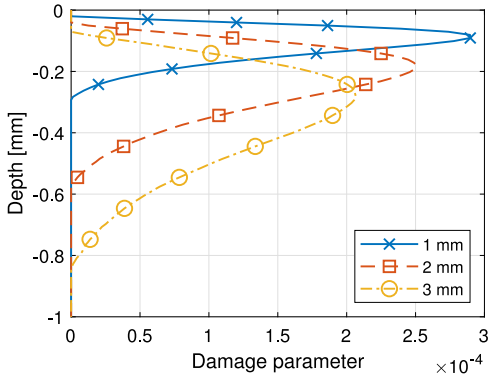

Fig. 13. Damage parameter for distributed impacts on epoxy targets for different droplet diameters at 80 m s^{-1} as a function of the z–coordinate for a constant number of impacts.

A functionally graded material led to a significantly reduced stress state in the coating layer due to more spread out reflections in the interphase region. The effect of interphase thickness on the predicted lifetime is shown for 3 mm droplet impacts on 250 μm TPUD60 and PAI coated epoxy substrates in Fig. 15. It can be seen that thicker interphases result in longer lifetimes. The effect is less than the effect of LEP thickness itself. A smart combination of a sufficiently thick LEP with a thick interphase could lead to a resilient material system that can withstand impacts with an average droplet size due to the LEP thickness and some impacts with larger droplets due to the interphase thickness.

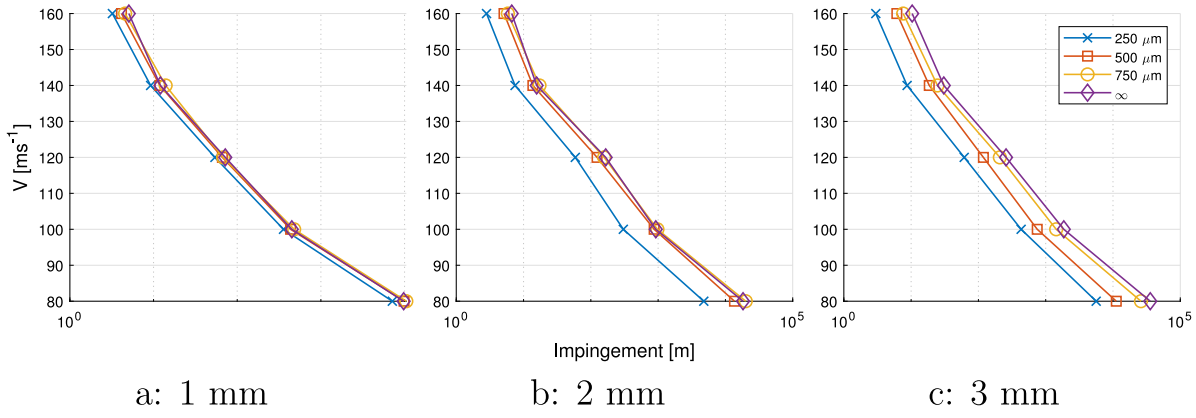

Fig. 14. The effect of LEP thickness and droplet diameter for PAI coated epoxy substrates on the resulting impingement lifetime.

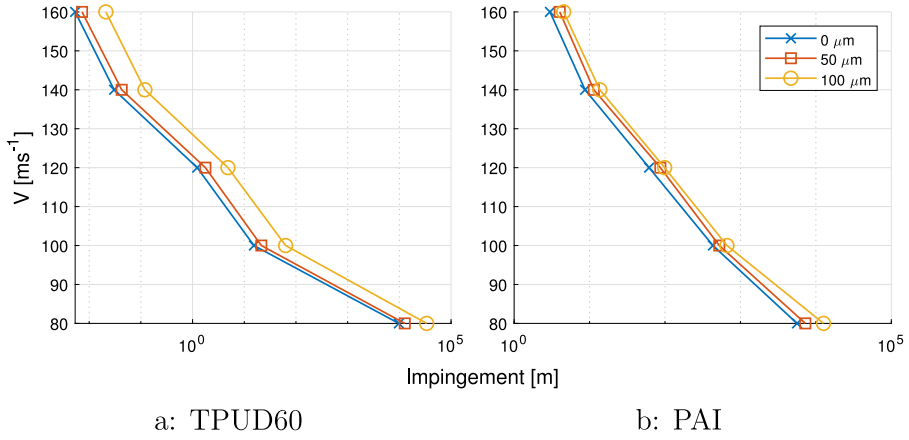

Fig. 15. The effect of interphase thickness on the lifetime of 250 μm TPUD60 and PAI coated epoxy substrates for 3 mm droplet diameter impacts.

3.3. The effect of fatigue strength parameters

Fig. 16 shows the sensitivity of the predicted lifetime of an epoxy target for 2 mm diameter liquid droplet impact with respect to changes in the fatigue parameters. It can be seen that a change in the ultimate tensile strength causes the predicted lifetime to be significantly influenced, especially at higher impact velocities. This has to do with the fact that high–cycle fatigue is occurring and the slope of the SN–curve significantly influences the lifetimes. A higher ultimate tensile strength has a significant effect on the slope of the VN–curve. The effect of σ_I is more prominent at lower impact velocities. This has to do with the fact that the involved stresses are lower and the endurance limit significantly influences the stress cycles involved in the fatigue analysis. The effect of N on the predicted lifetime is limited. The large effect of small changes in σ_U and σ_I emphasizes the need for proper high strain rate, high–cycle fatigue data in order to make accurate lifetime predictions.

The curves discussed above are based on the same stress cycle magnitudes and counts since they were stored after Rainflow counting. Therefore, the curves are deterministic and the study isolates the effect of a change in fatigue parameters. For different impact conditions, the Rainflow counting has to be performed an additional time and hence, the model becomes stochastic. For this reason, a Monte Carlo analysis was performed to show the spread in predicted lifetime as a function of the stochastic nature of the model. The results are shown in Fig. 17 for 2 mm diameter droplet impacts on an epoxy target with the number of impacts for each simulation n equal to 5.000. It can be seen that the standard deviations are low and the lifetime prediction results presented are stable and therefore valid. Interestingly, for lower impact velocities, the standard deviations are slightly higher than for higher impact velocities. This indicates that longer lifetimes are more difficult to predict. Since longer lifetimes are mainly driven by low stress magnitudes, overlap of low stress histories becomes more important. This is the case for low velocity impacts and the impact location distribution.

4. Discussion

Single point impact lifetime is driven by the maximum stress and its location in the coating–substrate system. This results in a straightforward coupling between fatigue lifetime and the stress field for constant impact velocity. If the impact velocity is changing, overlap of stress history regions occurs and the damage mechanisms and fatigue lifetime calculations become more complex.

For distributed impact locations, stress fields overlap even for a constant impact velocity. This can be understood from Fig. 9 because for distributed impacts, the damage does no longer occur at the marked point, but overlap of lower stress regions occurs causing more fatigue cycles. This results in a non-linear coupling between the stress state and the damage locations and lifetime of the materials. The method proposed for distributed impacts in the current work is based on a superposition of stress fields, the Rainflow counting algorithm and the Palmgren–Miner damage rule. This means that well established ideas can be used to predict the lifetimes and damage locations of distributed liquid droplet impacts on coated substrates.

It was shown that comparison of the predicted lifetimes for single point impacts and distributed impact locations is non–trivial due to this overlap. The overlapping area and the stress cycle magnitudes and counts depend on the impact, geometric and material parameters and the relation is not straightforward. Because of the fundamental

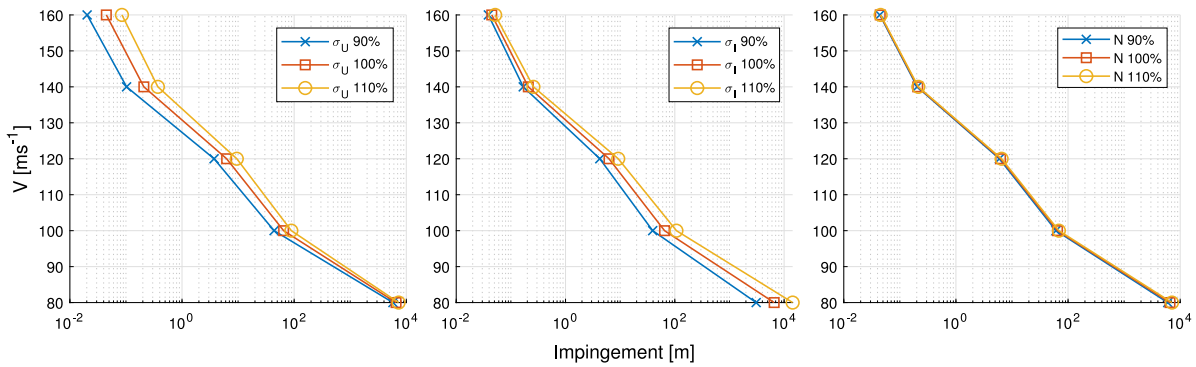

Fig. 16. Influence of changes in σ_U, σ_I and N on the impingement value for 2 mm diameter droplet impacts on an epoxy target.

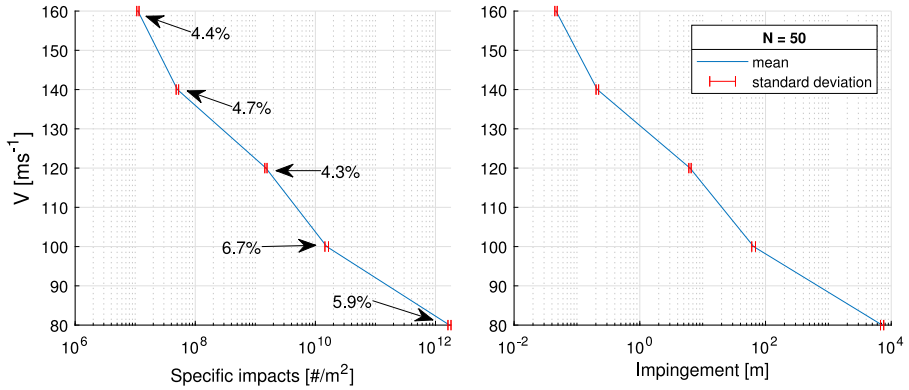

Fig. 17. Mean and standard deviation for the predicted lifetimes of a Monte Carlo simulation of 2 mm diameter droplet impacts on epoxy targets.

differences between single point and distributed impact locations, care should be taken when interpreting rain erosion test results from different test setups or facilities. This holds for tested lifetime values, but also for damage locations and types. The developed modeling framework could be used to relate the different loading cases since it includes the non–linear effects.

Fitting of the predicted VN–curves to measured fatigue parameters is challenging due to the fact that the VN–curve is not directly related to the SN–curve. The lifetime of the material is based on a combination of overlapping regions of low and high stresses, which means that changing fatigue parameters like σ_U, σ_I or N does not have the same effect in the VN–curve as it has in the SN–curve. A coupling exists based on the stress history through thickness. In order to couple the SN–curve to the VN–curve, it is therefore important to understand which stress magnitudes influence the lifetime and to what extend. These effects are included in the modeling framework.

There is not a straightforward relation between changes in impact or geometric parameters and the predicted lifetimes. This means that a change in droplet diameter, material parameters or even impact velocity does not necessarily result in a shift or change of slope in the lifetime curve but the behavior may be quite different. This is due to the fact that the change in stress field and the overlap of low stress regions for fatigue damage calculations is not trivial. The developed model includes the nonlinear effects which enables a more accurate prediction of the effects of changes in the LEP design on the lifetime.

High strain rate material parameters are very important to consider for accurate lifetime predictions. These high strain rate parameters do not only determine how the materials respond to liquid droplet impact and how the stress develops in the coating–substrate system but also how the material responds to fatigue loads. It was shown in literature [18] that at high strain rates, typical polymeric materials behave in a glassy way and the yield strength increases. This indicates that at the relevant strain rates for liquid droplet impact, the materials are loaded in the elastic regime and high–cycle fatigue is the relevant damage mechanism. The considered fatigue damage calculations should therefore focus on high strain rate, high–cycle material data. This material data is challenging to obtain since the required strain rates are in the order of 10^6 and high frequency fatigue tests lead to viscoelastic heating of the materials which influences the results. A good starting point could be to fit the model to a single rain erosion test and predict the trends for changes in problem parameters. The elastic response of the considered LEP materials can be measured by e.g. a split Hopkinson pressure bar experiment.

Since the problem concerns high–cycle fatigue, the initial state of the coating–substrate system is largely determining the fatigue lifetime. Any irregularities in the material could cause stress concentrations and growth of fatigue damage. This can lead to unpredictable behavior if the quality of the production process of the LEP system is not well controlled. Combined with the complex non–linear effects of the stress cycles in the material, these uncertainties could lead to seemingly random failure of the LEP system as sometimes observed in rain erosion experiments in literature [24].

5. Conclusions

Lifetime prediction of coated-substrates for wind turbine blade applications is traditionally based on the Springer model. The current work investigated the possibilities of using a numerical framework to predict the lifetimes and the influence of LEP design parameters on the predicted lifetimes. The liquid droplet impact pressure and coating–substrate stress history were modeled according to earlier work by the authors [20,21]. The lifetime prediction was based on the Palmgren–Miner rule and the Rainflow counting algorithm which were applied for each node. A method for distributed impacts was proposed based on a superposition of the stress histories.

The current work analyzed the effect of changes in LEP design parameters on the predicted rain erosion lifetime of the coating–substrate system. The effect of droplet diameter, LEP thickness, interphase thickness and coating material parameters was studied for single point impact locations and distributed impacts. It was shown that the stresses and the number of cycles in the material due to distributed impacts are highly non–linear due to overlap of stress history and dynamic stress fields caused by interactions of waves with interfaces/interphases. It was argued that high strain rate material parameters are required in order to accurately predict fatigue lifetimes and that the production process of the coating–substrate system should be controlled in order to limit initial defects which could accelerate fatigue damage growth. The following conclusions were drawn based on the work performed:

1. The droplet diameter significantly affects the lifetime of the coating substrate system.
   The initial contact point between the droplet and the substrate is most important for the stress and therefore the lifetime of the LEP system. Small droplets have a smaller volume than large droplets and hence, more impacts occur for the same impingement value for small droplets. Consequently, small droplets cause more damage than large droplets for the same impingement value for bulk materials.
2. The LEP thickness significantly influences the lifetime of the coated substrate.
   The design of the LEP system (especially the thickness of the coating layer) influences the stress state in the system and with that the expected lifetime. Thin coating layers cause reflections of high energy stress waves at the interface which lead to a significant increase in the stress level in the coating system and hence, a lower lifetime. This effect also depends on the droplet diameter since larger droplets have a larger influenced volume and the energy in the stress waves penetrates to a larger depth. Therefore, the LEP design should be based on site specific conditions at the blade tip which should be measured in the field [6] or modeled using rainfall kinematics [14,15]. The developed model can be utilized to optimize LEP design and study the sensitivity to changes in impact, geometric and material parameters on the performance of the LEP system.
3. There is a difference in lifetime and damage location for single point impacts and distributed impacts due to overlap of high–cycle fatigue regions.
   For distributed impacts, low stress regions overlap which leads to a higher number of cycles for these low stress regions. This leads to high–cycle fatigue damage in different areas than for single point impacts. This indicates that there is a significant difference in observed damage mechanisms and lifetimes between the different types of rain erosion tests that are used. This should be taken into account when interpreting rain erosion test results from different test types or facilities.
4. The lifetime model is very sensitive to changes in the used ultimate tensile strength.
   This dependence on ultimate tensile strength is related to the way the model incorporates the fatigue damage SN–curve. The ultimate tensile strength is used in Eq. (1) to model the SN–curve. Since the liquid droplet impact loading is mainly causing stresses in the elastic regime of the materials (at high strain rates), high–cycle fatigue methods should be used for damage calculations. The use of the ultimate tensile strength should therefore be prevented and the model is best fitted to high strain rate and high–cycle fatigue experiments.

Future research should be focused on obtaining high strain rate high–cycle fatigue parameters in order to couple the model to field data and rain erosion experiments. This can be a challenging task due to the high strain rates required ($\pm 10^6$ s^{-1}) and the lack of a standard test method. It would be useful to measure high strain rate elastic parameters (using e.g. a split Hopkinson pressure bar) and to fit the resulting model to a single rain erosion test to be able to study the effect of changes in impact and geometric parameters as well as site–specific performance.

Declaration of competing interest

The authors declare that they have no known competing financial interests or personal relationships that could have appeared to influence the work reported in this paper.

Data availability

Data will be made available on request.

Acknowledgments

This project is financed by TKI-Wind op Zee Topsector Energy subsidy from the Ministry of Economic Affairs of the Netherlands with the reference number TEWZ118008.

References

[1] Keegan MH, Nash DH, Stack MM. On erosion issues associated with the leading edge of wind turbine blades. J Phys D: Appl Phys 2013;46(38):383001. http://dx.doi.org/10.1088/0022-3727/46/38/383001.
[2] Springer GS. Erosion by liquid impact. John Wiley and Sons, New York, NY; 1976, p. 264.
[3] Eisenberg D, Laustsen S, Stege J. Wind turbine blade coating leading edge rain erosion model: Development and validation. Wind Energy 2018;21:942–51. http://dx.doi.org/10.1002/we.2200.
[4] Mishnaevsky L. Toolbox for optimizing anti-erosion protective coatings of wind turbine blades: Overview of mechanisms and technical solutions. Wind Energy 2019;22(11):1636–53. http://dx.doi.org/10.1002/we.2378.
[5] Hoksbergen N, Akkerman R, Baran I. The springer model for lifetime prediction of wind turbine blade leading edge protection systems: A review and sensitivity study. Materials 2022;15(3):1170. http://dx.doi.org/10.3390/ma15031170.
[6] Pryor SC, Barthelmie RJ, Cadence J, Dellwik E, Hasager CB, Kral ST, Reuder J, Rodgers M, Veraart M. Atmospheric drivers of wind turbine blade leading edge erosion: Review and recommendations for future research. Energies 2022;15(22):8553. http://dx.doi.org/10.3390/en15228553.
[7] Slot HM, Gelinck ERM, Rentrop C, Van der Heide E. Leading edge erosion of coated wind turbine blades: Review of coating life models. Renew Energy 2015;80:837–48. http://dx.doi.org/10.1016/j.renene.2015.02.036.
[8] Slot HM, IJzerman RM, le Feber M, Nord-Varhaug K, van der Heide E. Rain erosion resistance of injection moulded and compression moulded polybutylene terephthalate PBT. Wear 2018;414–415:234–42. http://dx.doi.org/10.1016/j.wear.2018.08.016.
[9] Slot H, Matthews D, Schipper D, van der Heide E. Fatigue-based model for the droplet impingement erosion incubation period of metallic surfaces. Fatigue Fract Eng Mater Struct 2021;44:199–211. http://dx.doi.org/10.1111/ffe.13352.
[10] Hu W, Chen W, Wang X, Jiang Z, Wang Y, Verma AS, Teuwen JJ. A computational framework for coating fatigue analysis of wind turbine blades due to rain erosion. Renew Energy 2021;170:236–50. http://dx.doi.org/10.1016/j.renene.2021.01.094.
[11] Doagou-Rad S, Mishnaevsky L. Rain erosion of wind turbine blades: computational analysis of parameters controlling the surface degradation. Meccanica 2020;55(4):725–43. http://dx.doi.org/10.1007/s11012-019-01089-x.
[12] Amirzadeh B, Louhghalam A, Raessi M, Tootkaboni M. A computational framework for the analysis of rain-induced erosion in wind turbine blades, part II: Drop impact-induced stresses and blade coating fatigue life. J Wind Eng Ind Aerodyn 2017;163(February):44–54. http://dx.doi.org/10.1016/j.jweia.2016.12.007.
[13] Doagou-Rad S, Mishnaevsky L, Bech JI. Leading edge erosion of wind turbine blades: Multiaxial critical plane fatigue model of coating degradation under random liquid impacts. Wind Energy 2020;23(8):1752–66. http://dx.doi.org/10.1002/we.2515.
[14] Shankar Verma A, Jiang Z, Ren Z, Caboni M, Verhoef H, Mijle-Meijer H, Castro SG, Teuwen JJ. A probabilistic long-term framework for site-specific erosion analysis of wind turbine blades: A case study of 31 dutch sites. Wind Energy 2021;24(11):1315–36. http://dx.doi.org/10.1002/we.2634.
[15] Verma AS, Jiang Z, Caboni M, Verhoef H, van der Mijle Meijer H, Castro SGP, Teuwen JJE. A probabilistic rainfall model to estimate the leading-edge lifetime of wind turbine blade coating system. Renew Energy 2021;178:1435–55. http://dx.doi.org/10.1016/j.renene.2021.06.122.

[16] Amirzadeh B, Louhghalam A, Raessi M, Tootkaboni M. A computational framework for the analysis of rain-induced erosion in wind turbine blades, part I: Stochastic rain texture model and drop impact simulations. J Wind Eng Ind Aerodyn 2017;163:33–43. http://dx.doi.org/10.1016/j.jweia.2016.12.006.

[17] Bech JI, Johansen NFJ, Madsen MB, Hannesdóttir Á, Hasager CB. Experimental study on the effect of drop size in rain erosion test and on lifetime prediction of wind turbine blades. Renew Energy 2022;197:776–89. http://dx.doi.org/10.1016/j.renene.2022.06.127.

[18] Walley SM, Field JE. Strain rate sensitivity of polymers in compression from low to high rates. DYMAT J 1994;1(3):211–27.

[19] Yi J, Boyce MC, Lee GF, Balizer E. Large deformation rate-dependent stress–strain behavior of polyurea and polyurethanes. Polymer 2006;47(1):319–29. http://dx.doi.org/10.1016/j.polymer.2005.10.107.

[20] Hoksbergen TH, Akkerman R, Baran I. Coating stress analysis for leading edge protection systems for wind turbine blades. In: Proceedings of the 20th European conference on composite materials - composites meet sustainability, Vol. 5. 2022, p. 113–20. http://dx.doi.org/10.5075/epfl-298799_978-2-9701614-0-0.

[21] Hoksbergen TH, Akkerman R, Baran I. Liquid droplet impact pressure on (elastic) solids for prediction of rain erosion loads on wind turbine blades. J Wind Eng Ind Aerodyn 2023;233:105319. http://dx.doi.org/10.1016/j.jweia.2023.105319.

[22] Hoksbergen N. Data underlying the publication: Fatigue lifetime prediction model for leading edge protection coating systems of wind turbine blades. 2023, http://dx.doi.org/10.4121/6bbd8d44-da88-402d-ac77-8adb8d5de069.v1.

[23] ASTM E1049-85: Standard practices for cycle counting in fatigue analysis. Tech. rep., ASTM; 2017, p. 10. http://dx.doi.org/10.1520/E1049-85R17.

[24] Katsivalis I, Chanteli A, Finnegan W, Young TM. Mechanical and interfacial characterisation of leading-edge protection materials for wind turbine blade applications. Wind Energy 2022;1–17. http://dx.doi.org/10.1002/we.2767.